Chai Y, Jiang X, Ito Y, Bringas Jr P, Han J, Rowitch DH, Soriano P, McMahon AP, Sucov HM. 2000. Fate of the mammalian cranial neural crest during tooth and mandibular morphogenesis. Development 127:1671–1679.

Cho MI, Garant PR. 1989. Radioautographic study of [3H]mannose utilization during cementoblast differentiation, formation of acellular cementum, and development of periodontal ligament principal fibers. Anat Rec 223:209–222.

Cho MI, Garant PR. 1996. Expression and role of epidermal growth factor receptors during differentiation of cementoblasts, osteoblasts, and periodontal ligament fibroblasts in the rat. Anat Rec 245:342–360.

Cho MI, Garant PR. 2000. Development and general structure of the periodontium. Periodontol 2000 24:9–27.

Danielson KG, Baribault H, Holmes DF, Graham H, Kadler KE, Iozzo RV. 1997. Targeted disruption of decorin leads to abnormal collagen fibril morphology and skin fragility. J Cell Biol 136:729–743.

Debby-Brafman A, Burstyn-Cohen T, Klar A, Kalcheim C. 1999. F-spondin, expressed in somite regions avoided by neural crest cells, mediates inhibition of distinct somite domains to neural crest migration. Neuron 22: 475–488.

Diekwisch TG. 2002. Pathways and fate of migratory cells during late tooth organogenesis. Connect Tissue Res 43:245–256.

Engler AJ, Sen S, Sweeney HL, Discher DE. 2006. Matrix elasticity directs stem cell lineage specification. Cell 126:677–689.

Everts V, Niehof A, Jansen D, Beertsen W. 1998. Type VI collagen is associated with microfibrils and oxytalan fibers in the extracellular matrix of periodontium, mesenterium and periosteum. J Periodontal Res 33:118–125.

Ezura Y, Chakravarti S, Oldberg A, Chervoneva I, Birk DE. 2000. Differential expression of lumican and fibromodulin regulate collagen fibrillogenesis in developing mouse tendons. J Cell Biol 151:779–788.

Fujii S, Maeda H, Wada N, Tomokiyo A, Saito M, Akamine A. 2008. Investigating a clonal human periodontal ligament progenitor/stem cell line in vitro and in vivo. J Cell Physiol 215:743–749.

Grzesik WJ, Narayanan AS. 2002. Cementum and periodontal wound healing and regeneration. Crit Rev Oral Biol Med 13:474–484.

Handa K, Saito M, Tsunoda A, Yamauchi M, Hattori S, Sato S, Toyoda M, Teranaka T, Narayanan AS. 2002a. Progenitor cells from dental follicle are able to form cementum matrix in vivo. Connect Tissue Res 43:406–408.

Handa K, Saito M, Yamauchi M, Kiyono T, Sato S, Teranaka T, Narayanan AS. 2002b. Cementum matrix formation in vivo by cultured dental follicle cells. Bone 31:606–611.

Horiuchi K, Amizuka N, Takeshita S, Takamatsu H, Katsuura M, Ozawa H, Toyama Y, Bonewald LF, Kudo A. 1999. Identification and characterization of a novel protein, periostin, with restricted expression to periosteum and periodontal ligament and increased expression by transforming growth factor beta. J Bone Miner Res 14:1239–1249.

Hou LT, Liu CM, Chen YJ, Wong MY, Chen KC, Chen J, Thomas HF. 1999. Characterization of dental follicle cells in developing mouse molar. Arch Oral Biol 44: 759–770.

Johnson RB. 1987. A classification of Sharpey's fibers within the alveolar bone of the mouse: a high-voltage electron microscope study. Anat Rec 217:339–347.

Kii I, Amizuka N, Minqi L, Kitajima S, Saga Y, Kudo A. 2006. Periostin is an extracellular matrix protein required for eruption of incisors in mice. Biochem Biophys Res Commun 342:766–772.

Kitagawa M, Kudo Y, Iizuka S, Ogawa I, Abiko Y, Miyauchi M, Takata T. 2006. Effect of F-spondin on cementoblastic differentiation of human periodontal ligament cells. Biochem Biophys Res Commun 349:1050–1056. Epub 2006 September 1051.

Klar A, Baldassare M, Jessell TM. 1992. F-spondin: a gene expressed at high levels in the floor plate encodes a secreted protein that promotes neural cell adhesion and neurite extension. Cell 69:95–110.

Kruzynska-Frejtag A, Wang J, Maeda M, Rogers R, Krug E, Hoffman S, Markwald RR, Conway SJ. 2004. Periostin is expressed within the developing teeth at the sites of epithelial–mesenchymal interaction. Dev Dyn 229:857–868.

Lekic P, Rojas J, Birek C, Tenenbaum H, McCulloch CA. 2001. Phenotypic comparison of periodontal ligament cells in vivo and in vitro. J Periodontal Res 36:71–79.

Liu SH, Yang RS, al-Shaikh R, Lane JM. 1995. Collagen in tendon, ligament, and bone healing. A current review. Clin Orthop Relat Res 318:265–278.

Luan X, Ito Y, Dangaria S, Diekwisch TG. 2006. Dental follicle progenitor cell heterogeneity in the developing mouse periodontium. Stem Cells Dev 15:595–608.

Lukinmaa PL, Waltimo J. 1992. Immunohistochemical localization of types I, V, and VI collagen in human permanent teeth and periodontal ligament. J Dent Res 71:391–397.

MacNeil RL, Berry JE, Strayhorn CL, Shigeyama Y, Somerman MJ. 1998. Expression of type I and XII collagen during development of the periodontal ligament in the mouse. Arch Oral Biol 43:779–787.

Matheson S, Larjava H, Hakkinen L. 2005. Distinctive localization and function for lumican, fibromodulin and decorin to regulate collagen fibril organization in periodontal tissues. J Periodontal Res 40:312–324.

McCulloch CA. 2000. Proteomics for the periodontium: current strategies and future promise. Periodontol 2000 40:173–183.

McCulloch CA, Lekic P, McKee MD. 2000. Role of physical forces in regulating the form and function of the periodontal ligament. Periodontol 2000 24:56–72.

Melcher AH, Cheong T, Cox J, Nemeth E, Shiga A. 1986. Synthesis of cementum-like tissue in vitro by cells cultured from bone: a light and electron microscope study. J Periodontal Res 21:592–612.

Morotome Y, Goseki-Sone M, Ishikawa I, Oida S. 1998. Gene expression of growth and differentiation factors-5, -6, and -7 in developing bovine tooth at the root forming stage (published erratum appears in Biochem Biophys Res Commun 1998 May 29;246(3):925). Biochem Biophys Res Commun 244:85–90.

Morsczeck C, Gotz W, Schierholz J, Zeilhofer F, Kuhn U, Mohl C, Sippel C, Hoffmann KH. 2005. Isolation of precursor cells (PCs) from human dental follicle of wisdom teeth. Matrix Biol 24:155–165. Epub 2005 February 2012.

Murakami Y, Kojima T, Nagasawa T, Kobayashi H, Ishikawa I. 2003. Novel isolation of alkaline phosphatase-positive subpopulation from periodontal ligament fibroblasts. J Periodontol 74:780–786.

Nanci A, Bosshardt DD. 2006. Structure of periodontal tissues in health and disease. Periodontol 2000 40:11–28.

Neidhardt J, Fehr S, Kutsche M, Lohler J, Schachner M. 2003. Tenascin-N: characterization of a novel member of the tenascin family that mediates neurite repulsion from hippocampal explants. Mol Cell Neurosci 23:193–209.

Nishida E, Sasaki T, Ishikawa SK, Kosaka K, Aino M, Noguchi T, Teranaka T, Shimizu N, Saito M. 2007. Transcriptome database KK-Periome for periodontal ligament development: expression profiles of the extracellular matrix genes. Gene 404:70–79. Epub 2007 September 2019.

Nojima N, Kobayashi M, Shionome M, Takahashi N, Suda T, Hasegawa K. 1990. Fibroblastic cells derived from bovine periodontal ligaments have the phenotypes of osteoblasts. J Periodontal Res 25:179–185.

Oliver G, Wehr R, Jenkins NA, Copeland NG, Cheyette BN, Hartenstein V, Zipursky SL, Gruss P. 1995. Homeobox genes and connective tissue patterning. Development 121:693–705.

Pitaru S, McCulloch CA, Narayanan SA. 1994. Cellular origins and differentiation control mechanisms during periodontal development and wound healing. J Periodontal Res 29:81–94.

Potten CS, Loeffler M. 1990. Stem cells: attributes, cycles, spirals, pitfalls and uncertainties. Lessons for and from the crypt. Development 110:1001–1020.

Rios H, Koushik SV, Wang H, Wang J, Zhou HM, Lindsley A, Rogers R, Chen Z, Maeda M, Kruzynska-Frejtag A, Feng JQ, Conway SJ. 2005. Periostin null mice exhibit dwarfism, incisor enamel defects, and an early-onset periodontal disease-like phenotype. Mol Cell Biol 25:11131–11144.

Saito M, Iwase M, Maslan S, Nozaki N, Yamauchi M, Handa K, Takahashi O, Sato S, Kawase T, Teranaka T, Narayanan AS. 2001. Expression of cementum-derived attachment protein in bovine tooth germ during cementogenesis. Bone 29:242–248.

Saito Y, Yoshizawa T, Takizawa F, Ikegame M, Ishibashi O, Okuda K, Hara K, Ishibashi K, Obinata M, Kawashima H. 2002. A cell line with characteristics of the periodontal ligament fibroblasts is negatively regulated for mineralization and Runx2/Cbfa1/Osf2 activity, part of which can be overcome by bone morphogenetic protein-2. J Cell Sci 115:4191–4200.

Saito M, Handa K, Kiyono T, Hattori S, Yokoi T, Tsubakimoto T, Harada H, Noguchi T, Toyoda M, Sato S, Teranaka T. 2005. Immortalization of cementoblast progenitor cells with Bmi-1 and TERT. J Bone Miner Res 20:50–57.

Salingcarnboriboon R, Yoshitake H, Tsuji K, Obinata M, Amagasa T, Nifuji A, Noda M. 2003. Establishment of tendon-derived cell lines exhibiting pluripotent mesenchymal stem cell-like property. Exp Cell Res 287:289–300.

Scadden DT. 2006. The stem-cell niche as an entity of action. Nature 441:1075–1079.

Sena K, Morotome Y, Baba O, Terashima T, Takano Y, Ishikawa I. 2003. Gene expression of growth differentiation factors in the developing periodontium of rat molars. J Dent Res 82:166–171.

Seo BM, Miura M, Gronthos S, Bartold PM, Batouli S, Brahim J, Young M, Robey PG, Wang CY, Shi S. 2004. Investigation of multipotent postnatal stem cells from human periodontal ligament. Lancet 364:149–155.

Shimono M, Ishikawa T, Ishikawa H, Matsuzaki H, Hashimoto S, Muramatsu T, Shima K, Matsuzaka K, Inoue T. 2003. Regulatory mechanisms of periodontal regeneration. Microsc Res Tech 60:491–502.

Somerman MJ, Ouyang HJ, Berry JE, Saygin NE, Strayhorn CL, D'Errico JA, Hullinger T, Giannobile WV. 1999. Evolution of periodontal regeneration: from the roots' point of view. J Periodontal Res 34:420–424.

Sunkin SM, Hohmann JG. 2007. Insights from spatially mapped gene expression in the mouse brain. Hum Mol Genet 16:209–219.

Ten Cate AR. 1994. Development of the periodontium. In: Ten Cate AR, editor. Oral histology, development, structure, and function. St. Louis, MO: Mosby. p 257–275.

Ten Cate AR, Mills C. 1972. The development of the periodontium: the origin of alveolar bone. Anat Rec 173:69–77.

Thesleff I, Keranen S, Jernvall J. 2001. Enamel knots as signaling centers linking tooth morphogenesis and odontoblast differentiation. Adv Dent Res 15:14–18.

Tzarfati-Majar V, Burstyn-Cohen T, Klar A. 2001. F-spondin is a contact-repellent molecule for embryonic motor neurons. Proc Natl Acad Sci USA 98:4722–4727.

Wolfman NM, Hattersley G, Cox K, Celeste AJ, Nelson R, Yamaji N, Dube JL, DiBlasio-Smith E, Nove J, Song JJ, Wozney JM, Rosen V. 1997. Ectopic induction of tendon and ligament in rats by growth and differentiation factors 5, 6, and 7, members of the TGF-beta gene family. J Clin Invest 100:321–330.

Yamada S, Murakami S, Matoba R, Ozawa Y, Yokokoji T, Nakahira Y, Ikezawa K, Takayama S, Matsubara K, Okada H. 2001. Expression profile of active genes in human periodontal ligament and isolation of PLAP-1, a novel SLRP family gene. Gene 275:279–286.

Yamada S, Tomoeda M, Ozawa Y, Yoneda S, Terashima Y, Ikezawa K, Ikegawa S, Saito M, Toyosawa S, Murakami S. 2007. PLAP-1/asporin, a novel negative regulator of periodontal ligament mineralization. J Biol Chem 282:23070–23080.

Yamashita Y, Sato M, Noguchi T. 1987. Alkaline phosphatase in the periodontal ligament of the rabbit and macaque monkey. Arch Oral Biol 32:677–678.

Yokoi T, Saito M, Kiyono T, Iseki S, Kosaka K, Nishida E, Tsubakimoto T, Harada H, Eto K, Noguchi T, Teranaka T. 2007. Establishment of immortalized dental follicle cells for generating periodontal ligament in vivo. Cell Tissue Res 327:301–311.

Yoshizawa T, Takizawa F, Iizawa F, Ishibashi O, Kawashima H, Matsuda A, Endo N, Kawashima H. 2004. Homeobox protein MSX2 acts as a molecular defense mechanism for preventing ossification in ligament fibroblasts. Mol Cell Biol 24:3460–3472.

J. Oral Biosci. 50(3) : 175-182, 2008

REVIEW (Developmental Biology of HERS and Tooth Root Formation)

Comprehensive Analysis of Tissue-specific Markers Involved in Periodontal Ligament Development

Masahiro Saito[§], Eisaku Nishida and Toshiyuki Yoneda

Department of Molecular and Cellular Biochemistry, Osaka University Graduate School of Dentistry
1-8 Yamadaoka, Suita, Osaka 565-0871, Japan
〔Received on April 21, 2008 ; Accepted on May 26, 2008〕

Key words : transcriptome／EST／periodontal ligament／extracellular matrix／development

Abstract : The periodontal ligament (PDL) is a tendon/ligament-like fibrous tissue that connects the tooth root surface and the alveolar bone. General interest has been expressed in PDL development as a model for connective tissue formation because of its ability to adapt to mechanical loading. PDL cell has its origin in the dental follicle (DF) cell, and it begins to differentiate during tooth root development. During apical development of the tooth root, PDL progenitors in DF differentiate into PDL cells to form the PDL ; however, the molecular mechanisms of PDL development have not yet been clarified, as PDL lineage-specific markers are not available. We recently established a transcriptome database for the human PDL (KK-Periome database), and screened the genes specifically expressed during PDL development. Initial screening of the database allowed us to identify F-spondin and tenascin-N, which are restricted to DF and PDL cells, respectively. Thus, these could serve as PDL lineage-specific markers that would be useful for investigating the molecular mechanisms of PDL development.

Introduction

The periodontal ligament (PDL) is a connective tissue capable of withstanding mechanical loading, such as occlusal force. Like most connective tissues, collagen type I is predominant, but collagen types III, IV, V, VI and XII and proteoglycans, which regulate collagen fibril formation, are also deposited in the PDL extracellular matrix (ECM)[1-3]. The cellular content of PDL is predominated by PDL cells which can form Sharpey's fibers, collagen fibers embedded in the calcified matrix[4]. The structure of PDL is often irreversibly damaged by the chronic inflammatory disease "periodontitis", which affects the periodontium[5]. Although various treatments are available for periodontitis, it is not yet possible to reliably regenerate the PDL[6-8]. To develop methods to regenerate the damaged PDL, a basic understanding of PDL development at the molecular level is required, as the regeneration process must mimic the cellular events of PDL development[9,10]. Recent advances have revealed that progenitor or stem cells are present in the adult PDL[11-13]. Hence, it is important to clarify the molecular basis of PDL regeneration from these stem cells or progenitors.

The molecular mechanisms of PDL development have not yet been clarified, as there is limited information on the genes related to the differentiation and lineage commitment of PDL progenitors[14]. However, recent advances in transcriptome database technology and the availability of human and mice genome sequences allow unlimited access to information

§ Corresponding author
E-mail : mssaito@dent.osaka-u.ac.jp

about genes potentially involved in the development of specialized tissue[15]. In this paper, we describe the methodology for screening PDL lineage-specific markers from the KK-Periome database, and discuss the significance of ECM components as markers for PDL development.

Periodontal Ligament Development

PDL cells originate from DF cells that contain an ectomesenchymal progenitor cell population derived from cranial neural crest cells[16]. As DF contains three kinds of progenitors, including cementoblast progenitors, PDL progenitors, and osteoblast progenitor, the developmental events of DF are of considerable interest (Fig. 1). During the tooth root-forming stage, cementoblast progenitors migrate to the surface of the tooth root and differentiate into cementoblasts to form the cementum matrix[17,18]. Almost at the same time, PDL progenitors differentiate into PDL on cementoblasts, inserting collagen fibers known as Sharpey's fibers into the cementum matrix. Fiber insertion also takes place along the alveolar bone. Finally, both bone- and PDL-derived fibers coalesce in the PDL to form the intermediate plexus, which is similar to tendinous tissue[14,19].

A recent study demonstrated that cultured mouse DF cells are capable of forming PDL-like tissue that shows a high expression of PDL formation-related genes, such as periostin and type XII collagen, upon implantation into immunodeficient mice[20]. In addition, a PDL progenitor-like cell line that could not form mineralized nodules was isolated from cultured DF cells, thus suggesting that PDL lineage-committed progenitors are present among DF cells[21—23]. Although not well characterized at the molecular level, investigation of DF cell differentiation into PDL cells made it possible to clarify PDL development ; however, the precise differentiation mechanisms of DF cells remain poorly understood due to limited information on specific marker genes for PDL lineage commitment. Identification of PDL lineage-specific markers throughout the course of DF cell differentiation is thus important.

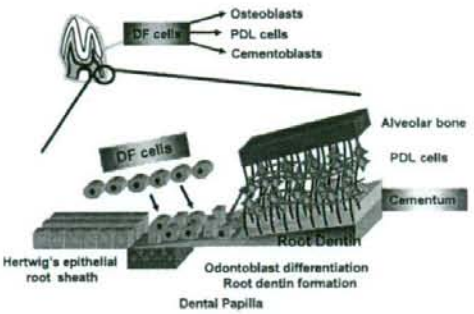

Fig. 1 Schematic model of PDL development
DF cells are composed of ectomesenchymal progenitors for the periodontal ligament, cementoblasts and osteoblasts. After tooth root formation, cementoblast progenitors migrate onto the tooth root surface and then differentiate into cementoblasts. At the same time, PDL progenitors differentiate to form PDL cells, and Sharpey's fiber insertion into cementum occurs. Osteoblast progenitors also differentiate into osteoblasts to produce the bony socket wall. Finally, both bone- and PDL-derived fibers coalesce in the PDL to form the intermediate plexus.

Establishment of KK-Periome Database

For identification of PDL lineage-specific markers, we established the KK-Periome database, which is a collection of expressed sequence tags (ESTs) that are strongly expressed in human PDL[24]. ESTs are short, single-pass sequence reads of randomly selected clones from a cDNA library, and are invaluable for identifying genes and gene expression patterns in particular types of tissue[25]. Thus, an EST database may provide a platform for identifying PDL specific-markers. It was previously reported that PDL possessed a stem cell population that can differentiate into PDL cells, osteoblasts and adipocytes[12]. We also reported that a progenitor able to form PDL tissue was present in DF and PDL[11,23]. From these findings, we hypothesized that both differentiated PDL-specific and immature PDL-specific markers could be identified from the EST database of PDL.

In order to construct an EST database for human

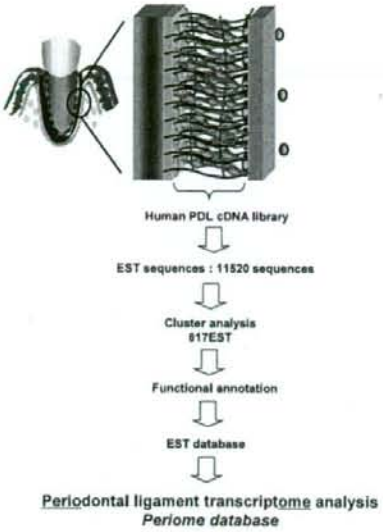

Fig. 2 Strategy for construction of KK-Periome database

The KK-Periome database is a collection of 617 clusters of expressed sequence tags (ESTs) that are highly expressed in human PDL cells. These EST clusters were derived from short sequence analysis of 11,520 randomly selected clones from a human PDL cDNA library. The 617 ESTs were classified according to their ontological function.

PDL, we compiled a cDNA library from the PDL and sequenced 11,520 cDNA clones. The resulting sequence data was assembled into 617 EST clusters, and these comprised the KK-Periome database (Fig. 2). As expected, the most abundantly expressed genes in the KK-Periome database were type I collagen and type III collagen, which are the major fibrillar collagens in PDL[26]. Seven genes with particularly high expression in PDL are SPARC, periostin, lumican, osteopontin, decorin, fibronectin, and PLAP-1/Asporin[27–30]. This expression profile was similar to the previous PDL-EST database[29]. Thus, the KK-Periome database reflects the PDL phenotype.

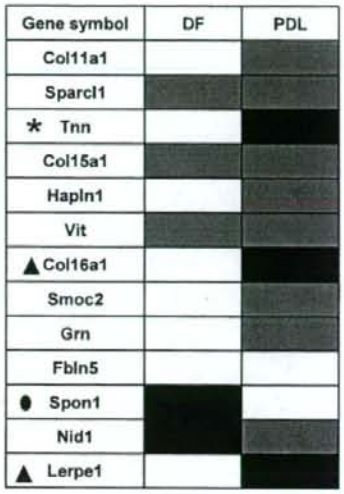

Fig. 3 Expression pattern analysis of 13 ECMs in DF cells and PDL cells

The expression patterns of 13 ECM clusters were investigated in DF cells and PDL cells by *in situ* hybridization analysis. Note that F-spondin (Spon1) is intensely expressed in DF cells (circle). In contrast, tenascin-N (Tnn) is strongly expressed in PDL cells (asterisk). Type XVI collagen (Col16a1) and leprecan (Lerpe1) are strongly expressed in PDL cells ; however, they are also expressed in odontoblasts (triangles). Black : strongly positive expression ; Gray : weakly positive expression ; White : no expression.

Screening of PDL Lineage-specific Genes

From the KK-Periome database, PDL lineage-specific markers were screened by two different parameters, functional classification and expression pattern : (1) As ECM is involved in the specificity of PDL cells, a potential PDL-specific marker was obtained from ECM clusters in the KK-Periome database ; (2) Candidate genes that may play critical roles in the

process of PDL development were selected by expression pattern on *in situ* hybridization analysis in mouse DF cells and adult PDL cells. As a result of screening, 13 EST clusters were obtained as candidates. These included collagen type XI alpha 1 (*COL11A1*), SPARC-like 1 (*SPARCL1*), tenascin-N (*TNN*), collagen type XV alpha 1 (*COL15A1*), hyaluronan and proteoglycan link protein 1 (*HAPLN1*), vitrin (*VIT*), type XVI collagen alpha 1 (*COL16A1*), SPARC-related modular calcium binding 2 (*SMOC2*), granulin (*GRN*), fibulin 5 (*FBLN5*), F-spondin (*SPON1*), nidogen 1 (*NID1*), and leprecan 1 (*LERPE1*) (Fig. 3). In the final step, we examined and compared gene expression in DF cells during the late bell stage of the tooth germ, and in PDL cells of the adult periodontium by *in situ* hybridization analysis. Among the candidate genes, F-spondin was expressed specifically in DF cells, and no expression was seen in other cell types in the late bell stage of the tooth germ, thus suggesting that F-spondin could serve as a DF marker. Nidogen 1 was also intensely expressed in DF cells, as well as in odontoblasts. The remaining candidate genes showed weak or no expression in DF cells, while they were expressed in other cells of the tooth germ. In PDL cells, the expression patterns of candidate genes were significantly different from those in DF cells. Expression of F-spondin and nidogen 1 was markedly lower in adult PDL cells, whereas the expression of tenascin-N, type XVI collagen alpha 1, and leprecan was markedly up-regulated. Among the up-regulated genes, tenascin-N was highly restricted to PDL cells, indicating that it could serve as a PDL marker.

F-spondin and Tenascin-N Serve as PDL Lineage-specific Markers

As a result of screening, F-spondin and tenascin-N were identified as candidate PDL lineage-specific markers. To test this possibility, we examined the expression patterns of F-spondin and tenascin-N during PDL development. F-spondin was initially expressed in the cap stage of DF cells and became progressively evident in the bell stage of DF cells ; however, the expression of F-spondin was significantly down-regulated in DF cells after birth, and no expression was observed in adult PDL cells. In contrast, the expression of tenascin-N could not be detected in the DF cells of developing tooth germs in the embryo, but was intensely up-regulated in adult PDL cells. Based on these observations, we believe that F-spondin and tenascin-N could serve as PDL lineage-specific markers for distinguishing DF cells from PDL cells (Fig. 4).

We then investigated whether F-spondin and tenascin-N are involved in the differentiation of PDL cells. Previous work has demonstrated that differentiation of cultured human PDL (hPDL) cells is induced upon implantation into immunodeficient mice[11,12]. Interestingly, tenascin-N expression was significantly induced in hPDL cells upon implantation while no expression was observed in *in vitro* cultured cells. These data suggest that hPDL cells express tenascin-N as a result of differentiation. Expression pattern analysis during PDL development agreed with the results of the *in vivo* differentiation study, thus suggesting that tenascin-N is a useful marker for differentiated PDL cells. In contrast to tenascin-N, the expression of F-spondin expression levels did not change after implantation into SCID mice. This is consistent with the notion that F-spondin may be involved in the initial process of PDL formation. Thus, F-spondin may play a role in the early stages of PDL formation, as demonstrated by *in situ* hybridization analysis during tooth germ development.

F-spondin Serves as DF Marker

F-spondin is an ECM-attached protein observed in the embryonic floor plate of vertebrates[31,32] and the caudal somite of birds[33], playing a dual role in the patterning of the nervous system. It promotes the adhesion and outgrowth of axons but inhibits adhesion of neural crest cells. Recent evidence suggests that F-spondin may act as a regulator of amyloid precursor protein (APP) processing[34]. Specifically, F-spondin binds to the extracellular domain of APP and inhibits β-secretase cleavage. Thus, F-spondin serves as a regulator of neuronal development, and is related to the onset of Alzheimer's disease. F-spondin also

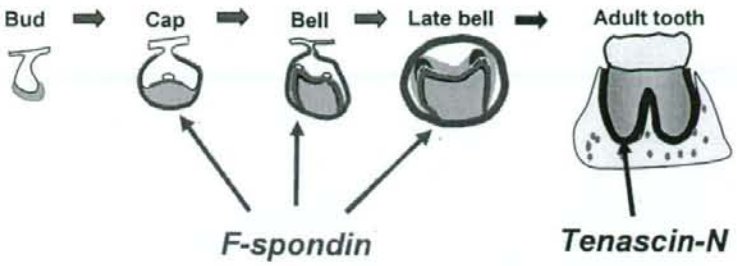

Fig. 4 F-spondin and tenascin-N serve as PDL lineage-specific markers
F-spondin is specifically expressed in DF during the cap, bell and late bell stages of the tooth germ ; however, its expression was significantly down-regulated in PDL cells. In contrast, the expression of tenascin-N was strongly induced in PDL cells of adult teeth. Thus, F-spondin and tenascin-N may serve as PDL lineage-specific markers that can distinguish DF cells and PDL cells.

appears to be involved in the formation of the periodontium during tooth development. Kitagawa *et al.* reported that F-spondin is strongly expressed in an immortalized human cementoblast cell line, and an overexpression study revealed that it affected cementoblast/osteoblast differentiation[35]. Immunohistochemical staining revealed that F-spondin protein was deposited in the cementum matrix. In contrast to these results, we showed that F-spondin may play a role in the early stages of PDL formation, as demonstrated by the presence of high F-spondin mRNA levels in DF cells, which subsequently decreases dramatically in adult PDL cells (Fig. 4). Although the precise function of F-spondin during tooth germ development is not yet clear, F-spondin expression was observed in dermal papilla cells. Numerous ectodermal tissues, such as teeth and hair, share similar epithelial-mesenchymal interactions during early development[36] ; therefore, the signaling molecules involved in ectodermal organogenesis may regulate the expression of F-spondin.

Tenascin-N Is Expressed in Differentiated PDL Cells

Tenascin-N was identified as a novel member of the tenascin family that is expressed in the adult brain, kidney and spleen. Contrary to other tenascins, tenascin-N is strongly expressed in neurons rather than glial cells in the central nervous system[37]. Interestingly, tenascin-N is strongly expressed in PDL cells, while no expression was observed in DF cells (Fig. 4). Most ECMs reported for PDL cells are expressed in both DF cells and PDL cells. For instance, periostin and PLAP1/Asporin were strongly expressed in DF cells, as well as in PDL cells[38,39]. Thus, tenascin-N may serve as a marker for terminally differentiated PDL cells. Tenascin-N expression was also detected in costal perichondrocytes, which form ligament tissue, thus suggesting that tenascin-N is associated with ligament tissue formation[24].

Concluding Remarks

In summary, a combination of the establishment of the KK-Periome database and *in situ* hybridization screening helped to identify PDL lineage-specific markers that would be useful for investigating PDL development. The development of PDL is associated with the change in the expression of ECM components. Among these, F-spondin and tenascin-N appear to be PDL lineage-specific markers. Further investigation is necessary to verify the actual function of these proteins/genes. Nevertheless, spatial and temporal expression analysis indicated that F-spondin and tenascin-N are related to the PDL differentiation process during development of the PDL lineage. Consequently, the molecular mechanisms of

PDL development will be better understood based on PDL lineage-specific markers, and therapeutic targets for the treatment of periodontal disease may be identified.

Acknowledgements

We would like to thank Drs. Nobuyoshi Shimizu and Takashi Sasaki for assistance with establishing the gene expression profiling database. We are also grateful to Dr. Toshio Teranaka and all the members of the Department of Molecular and Cellular Biochemistry, Osaka University School of Dentistry. This work was supported by a Grant-in-Aid for a High-Tech Research Center Project from the Ministry of Education, Culture, Sports, Science and Technology (MEXT) of Japan, the AGU High-Tech Research Center Project, the 2003 Multidisciplinary Research Project from MEXT, and grants from MEXT.

References

1) MacNeil, R. L., Berry, J. E., Strayhorn, C. L., Shigeyama, Y. and Somerman, M. J. : Expression of type I and XII collagen during development of the periodontal ligament in the mouse. Arch. Oral Biol. **43** : 779—787, 1998.
2) Everts, V., Niehof, A., Jansen, D. and Beertsen, W. : Type VI collagen is associated with microfibrils and oxytalan fibers in the extracellular matrix of periodontium, mesenterium and periosteum. J. Periodontal Res. **33** : 118—125, 1998
3) Lukinmaa, P. L. and Waltimo, J. : Immunohistochemical localization of types I, V, and VI collagen in human permanent teeth and periodontal ligament. J. Dent. Res. **71** : 391—397, 1992.
4) McCulloch, C. A., Lekic, P. and McKee, M. D. : Role of physical forces in regulating the form and function of the periodontal ligament. Periodontology **24** : 56—72, 2000.
5) Bartold, P. and Narayanan, A. : Molecular and cell biology of healthy and diseased periodontal tissues. Periodontology **40** : 29—49, 2006.
6) Somerman, M. J., Ouyang, H. J., Berry, J. E., Saygin, N. E., Strayhorn, C. L. D'Errico, J. A., Hullinger, T. and Giannobile, W. V. : Evolution of periodontal regeneration : from the roots' point of view. J. Periodontal Res. **34** : 420—424, 1999.
7) Melcher, A. H., Cheong, T., Cox, J., Nemeth, E. and Shiga, A. : Synthesis of cementum-like tissue *in vitro* by cells cultured from bone : a light and electron microscope study. J. Periodontal Res. **21** : 592—612, 1986.
8) Bartold, P. M., McCulloch, C. A., Narayanan, A. S. and Pitaru, S. : Tissue engineering : a new paradigm for periodontal regeneration based on molecular and cell biology. Periodontology **24** : 253—269, 2000.
9) Grzesik, W. J. and Narayanan, A. S. : Cementum and periodontal wound healing and regeneration. Crit. Rev. Oral Biol. Med. **13** : 474—484, 2002.
10) Shimono, M., Ishikawa, T., Ishikawa, H., Matsuzaki, H., Hashimoto, S., Muramatsu, T., Shima, K., Matsuzaka, K. and Inoue, T. : Regulatory mechanisms of periodontal regeneration. Microsc. Res. Tech. **60** : 491—502, 2003.
11) Handa, K., Saito, M., Yamauchi, M., Kiyono, T., Sato, S., Teranaka, T. and Narayanan, A. S. : Cementum matrix formation *in vivo* by cultured dental follicle cells. Bone **31** : 606—611, 2002.
12) Seo, B. M., Miura, M., Gronthos, S., Bartold, P. M., Batouli, S., Brahim, J., Young, M., Robey, P. G., Wang, C. Y. and Shi, S. : Investigation of multipotent postnatal stem cells from human periodontal ligament. Lancet **364** : 149—155, 2004.
13) Fujii, S., Maeda, H., Wada, N., Tomokiyo, A., Saito, M. and Akamine, A. : Investigating a clonal human periodontal ligament progenitor/stem cell line *in vitro* and *in vivo*. J. Cell Physiol. **215** : 743—749, 2008.
14) Cho, M. I. and Garant, P. R. : Development and general structure of the periodontium. Periodontology **24** : 9—27, 2000.
15) Sunkin, S. M. and Hohmann, J. G. : Insights from spatially mapped gene expression in the mouse brain. Hum. Mol. Genet. **16** : 209—219, 2007.
16) Chai, Y., Jiang, X., Ito, Y., Bringas, P., Jr., Han, J., Rowitch, D. H., Soriano, P., McMahon, A. P. and Sucov, H. M. : Fate of the mammalian cranial neural crest during tooth and mandibular morphogenesis. Development **127** : 1671—1679, 2000.
17) Saito, M., Iwase, M., Maslan, S., Nozaki, N., Yamauchi, M., Handa, K., Takahashi, O., Sato, S., Kawase, T., Teranaka, T. and Narayanan, A. S. : Expression of cementum-derived attachment protein in bovine tooth germ during cementogenesis. Bone **29** : 242—248, 2001.

18) Bosshardt, D. D. and Schroeder, H. E. : Cementogenesis reviewed : a comparison between human premolars and rodent molars. Anat. Rec. **245** : 267—292, 1996.
19) Ten Cate, A. R. : Development of the periodontium. In : Oral histology, development, structure, and function. (ed. Ten Cate, A. R.), pp.257—275, Mosby. St. Louis, 1994.
20) Yokoi, T., Saito, M., Kiyono, T., Iseki, S., Kosaka, K., Nishida, E., Tsubakimoto, T., Harada, H., Eto, K., Noguchi, T. and Teranaka, T. : Establishment of immortalized dental follicle cells for generating periodontal ligament *in vivo*. Cell Tissue Res. **327** : 301—311, 2007.
21) Morsczeck, C., Gotz, W., Schierholz, J., Zeilhofer, F., Kuhn, U., Mohl, C., Sippel, C. and Hoffmann, K. H. : Isolation of precursor cells (PCs) from human dental follicle of wisdom teeth. Matrix Biol. **24** : 155—165, 2005.
22) Luan, X., Ito, Y., Dangaria, S. and Diekwisch, T. G. : Dental follicle progenitor cell heterogeneity in the developing mouse periodontium. Stem Cells Dev. **15** : 595—608, 2006.
23) Saito, M., Handa, K., Kiyono, T., Hattori, S., Yokoi, T., Tsubakimoto, T., Harada, H., Noguchi, T., Toyoda, M., Sato, S. and Teranaka, T. : Immortalization of cementoblast progenitor cells with Bmi-1 and TERT. J. Bone Miner. Res. **20** : 50—57, 2005.
24) Nishida, E., Sasaki, T., Ishikawa, S. K., Kosaka, K., Aino, M., Noguchi, T., Teranaka, T., Shimizu, N. and Saito, M. : Transcriptome database KK-Periome for periodontal ligament development : expression profiles of the extracellular matrix genes. Gene **404** : 70—79, 2007.
25) Venter, J. C., Levy, S., Stockwell, T., Remington, K., and Halpern, A. : Massive parallelism, randomness and genomic advances. Nat. Genet. **33** Suppl : 219—227, 2003.
26) Lukinmaa, P. L., Vaahtokari, A., Vainio, S., Sandberg, M., Waltimo, J. and Thesleff, I. : Transient expression of type III collagen by odontoblasts : developmental changes in the distribution of pro-alpha 1 (III) and pro-alpha 1 (I) collagen mRNAs in dental tissues. Matrix **13** : 503—515, 1993.
27) Takano-Yamamoto, T., Takemura, T., Kitamura, Y. and Nomura, S. : Site-specific expression of mRNAs for osteonectin, osteocalcin, and osteopontin revealed by *in situ* hybridization in rat periodontal ligament during physiological tooth movement. J. Histochem. Cytochem. **42** : 885—896, 1994.
28) Horiuchi, K., Amizuka, N., Takeshita, S., Takamatsu, H., Katsuura, M., Ozawa, H., Toyama, Y., Bonewald, L. F. and Kudo, A. : Identification and characterization of a novel protein, periostin, with restricted expression to periosteum and periodontal ligament and increased expression by transforming growth factor beta. J. Bone Miner. Res. **14** : 1239—1249, 1999.
29) Yamada, S., Murakami, S., Matoba, R., Ozawa, Y., Yokokoji, T., Nakahira, Y., Ikezawa, K., Takayama, S., Matsubara, K. and Okada, H. : Expression profile of active genes in human periodontal ligament and isolation of PLAP-1, a novel SLRP family gene. Gene **275** : 279—286, 2001.
30) Matheson, S., Larjava, H. and Hakkinen, L. : Distinctive localization and function for lumican, fibromodulin and decorin to regulate collagen fibril organization in periodontal tissues. J. Periodontal Res. **40** : 312—324, 2005.
31) Klar, A., Baldassare, M. and Jessell, T. M. : F-spondin : a gene expressed at high levels in the floor plate encodes a secreted protein that promotes neural cell adhesion and neurite extension. Cell **69** : 95—110, 1992.
32) Tzarfati-Majar, V., Burstyn-Cohen, T. and Klar, A. : F-spondin is a contact-repellent molecule for embryonic motor neurons. Proc. Natl. Acad. Sci. USA **98** : 4722—4727, 2001.
33) Debby-Brafman, A., Burstyn-Cohen, T., Klar, A. and Kalcheim, C. : F-Spondin, expressed in somite regions avoided by neural crest cells, mediates inhibition of distinct somite domains to neural crest migration. Neuron **22** : 475—488, 1999.
34) Ho, A. and Sudhof, T. C. : Binding of F-spondin to amyloid-beta precursor protein : a candidate amyloid-beta precursor protein ligand that modulates amyloid-beta precursor protein cleavage. Proc. Natl. Acad. Sci. USA **101** : 2548—2553, 2004.
35) Kitagawa, M., Kudo, Y., Iizuka, S., Ogawa, I., Abiko, Y., Miyauchi, M. and Takata, T. : Effect of F-spondin on cementoblastic differentiation of human periodontal ligament cells. Biochem. Biophys. Res. Commun. **349** : 1050—1056, 2006.
36) Pispa, J. and Thesleff, I. : Mechanisms of ectodermal organogenesis. Dev. Biol. **262** : 195—205, 2003.
37) Neidhardt, J., Fehr, S., Kutsche, M., Lohler, J. and Schachner, M. : Tenascin-N : characterization of a novel member of the tenascin family that mediates neurite repulsion from hippocampal explants. Mol.

Cell Neurosci. **23** : 193—209, 2003.

38) Kruzynska-Frejtag, A., Wang, J., Maeda, M., Rogers, R., Krug, E., Hoffman, S., Markwald, R. R. and Conway, S. J. : Periostin is expressed within the developing teeth at the sites of epithelial-mesenchymal interaction. Dev. Dyn. **229** : 857—868, 2004.

39) Yamada, S., Tomoeda, M., Ozawa, Y., Yoneda, S., Terashima, Y., Ikezawa, K., Ikegawa, S., Saito, M., Toyosawa, S. and Murakami, S. : PLAP-1/asporin, a novel negative regulator of periodontal ligament mineralization. J. Biol. Chem. **282** : 23070—23080, 2007.

Colloids and Surfaces B: Biointerfaces 66 (2008) 71–76

Contents lists available at ScienceDirect

Colloids and Surfaces B: Biointerfaces

journal homepage: www.elsevier.com/locate/colsurfb

Synthesis of bone formation deriving biosilanes

Norio Yoshino[a,b,*], Kaori Nakajima[a], Keisuke Nakamura[a], Yukishige Kondo[a,b], Katsura Ohashi[c], Tomotaro Nihei[c], Masahiro Saito[d], Toshio Teranaka[c]

[a] Department of Industrial Chemistry, Faculty of Engineering, Tokyo University of Science, 12-1 Ichigaya-Funagawara, Shinjuku, Tokyo 162-0826, Japan
[b] Division of Colloid and Interface Science, Research Institute for Science and Technology, Tokyo University of Science, 1-3 Kagurazaka, Shinjuku, Tokyo 162-8601, Japan
[c] Department of Oral Medicine, Division of Restorative Dentistry, Kanagawa Dental College, 82 Inaoka-cho, Yokosuka, Kanagawa 238-8580, Japan
[d] Department of Biochemistry, Graduate School of Dentistry, Osaka University, 1-8 Yamadaoka, Suita, Osaka 565-0871, Japan

ARTICLE INFO

Article history:
Received 25 February 2008
Accepted 17 May 2008
Available online 24 May 2008

Keywords:
Silane coupling agent having amide group
Biosilane
Bone formation
Cell affinity
Surface modification

ABSTRACT

Six silane coupling agents having amide group (biosilanes) were synthesized with the aim to construct the material surface that allows cells to be compatible with it without their destruction. These agents were expected to make a soft landing to cytoplasm through the hydrogen bonding between their amide groups and cells. Evaluations of cell affinity using glass substrates modified with the synthesized biosilanes revealed that many cells remain on the modified glass plate. In addition, the implantation into the body of immunodeficient mouse of a composite material composed of porous hydroxyapatite and osteoblast showed the formation of a bone-like structure.

1. Introduction

The treatment using mainly autogenous bone graft or artificial material is now performed to cure bone defect parts. There are certain problems involved in the treatment using artificial material, however, such as deterioration in the body of the material and foreign body reaction in which the body recognizes it as a foreign matter. In recent years, much attention has been paid to reproductive medical treatment that allows regeneration of patient's own tissues in the body. Reproductive medical treatment is said to have many advantages including shortened period of treatment, reduction of biomaterial damage, and suppression of foreign body reaction [1–4].

We have synthesized a large number of silane coupling agents and studied the synthesized compounds as surface modifying agent [5–11]. In particular, fluorinated silane coupling agents have been shown to be greatly effective in preventing dental caries and periodontosis, while fluorinated aromatic silane coupling agents have been proved to be unique compounds at present that are usable in thermal nanoimprinting and high-temperature mold releasing as releasing agent heat-resistant up to 350 °C [11].

The present paper describes the synthesis of highly biocompatible and bone formative surface modifying agents for the development of materials used in medical treatment and the examination of cell affinity with the material surface modified with the compounds synthesized. The six surface modifying agents synthesized are amide group-containing silane coupling agents (biosilanes). Note here that amide group, a constituent of proteins, is hydrogen bond formative [12]. After hydroxyapatite (porous), the main component of bone, was treated with a synthesized biosilane, an inorganic/organic composite material with osteoblasts on the biosilane-modified surface was prepared and used in animal experiments. Scheme 1 shows the chemical structures of the biosilanes synthesized in the present work. TI9M was synthesized to study the effect of the silane coupling agent with no N–H bond on cell affinity.

2. Experimental

2.1. Materials

Trimethoxysilane (Tokyo Chemical Ind.) was used after being purified by distillation over calcium hydride (bp 81 °C). Chloroplatinic acid hexahydrate (H_2PtCl_6) (Kojima Chemicals) was used as 0.1 M solution in tetrahydrofuran (THF). THF was used after being

* Corresponding author at: Department of Industrial Chemistry, Faculty of Engineering, Tokyo University of Science, 12-1 Ichigaya-Funagawara, Shinjuku, Tokyo 162-0826, Japan. Tel.: +81 3 5228 8308; fax: +81 3 3235 2214.
E-mail addresses: yoshino@ci.kagu.tus.ac.jp, yoshinonorio2005@yahoo.co.jp (N. Yoshino).

0927-7765/$ – see front matter © 2008 Elsevier B.V. All rights reserved.
doi:10.1016/j.colsurfb.2008.05.009

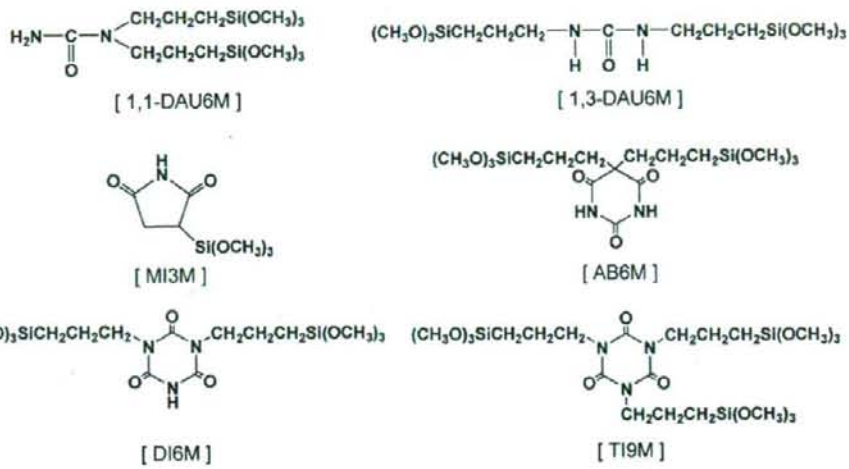

Scheme 1.

dehydrated over calcium hydride and distilled. 1,1-Diallylurea, 1,3-diallylurea, maleimide, allobarbital, diallylisocyanurate, and triallylcyanurate were used after being dried in a vacuum. The other reagents were used as supplied.

Microcover glass (12 mm × 12 mm × 0.17 mm) (Matsunami Glass Ind.), poly-L-lysine-modified cover glass (Rikaken), and 24-well plate (Falcon) were used as purchased. Phosphate buffer solution (PBS) was prepared by dissolving NaCl (8.0 g), KCl (0.2 g), Na_2HPO_4 (1.15 g), and KH_2PO_4 (0.2 g) in 1000 ml of distilled water and the resultant solution was used after being sterilized in an autoclave. Trypsin/ethylenediamine tetraacetic acid (EDTA) solution was prepared by adding 0.25 vol.% trypsin (GIBCO) to 1 mM aqueous EDTA solution (Wako Pure Chemicals). Culture medium was prepared in a clean bench by adding 10 wt% fetal bovine serum (BioWhittaker), 50 μg/ml ascorbic acid, and each of streptomycin and penicillin at 100 units/ml to minimum essential medium (Sigma). Luciferase assay reagent was prepared by mixing equal volumes of CellTiter-Glo buffer and CellTiter-Glo substrate (both from Promega). KUSA cells (mouse osteoblasts) cultured at 37 °C in a shallow dish were rinsed once with PBS after the supernatant of the culture medium was removed by sucking. After adding 4 ml of trypsin/EDTA solution and exfoliating the cells from the dish, the cells were transferred to a centrifuge tube containing 4 ml of the culture medium. The cells settled by centrifugation (1500 rpm, 5 min) were dispersed in 10 ml of the culture medium and the dispersion was diluted with the medium to give a concentration of 2×10^4 cells/ml. KUSA cell dispersion thus prepared was used to evaluate the cell affinity of the glass surface modified with biosilane.

Hydroxyapatite powder (Hap) (single crystal, Wako) used in FT-IR analysis was used as purchased. Male 5-week-old immunodeficient mice (Nihon Kurea) and β-TCP (75% porosity, pore size 100–400 μm) (Olympus) were used as supplied in transplantation experiment.

2.2. Measurements

FT-IR spectrum was measured by the attenuated total reflection (ATR) method using a Nicolet Avatar 360 FT-IR spectrometer. A Bruker DPX-400 spectrometer was used to measure 400 MHz ^1H NMR spectrum in $CDCl_3$ at room temperature with TMS as internal standard. A JEOL JMS SX102A was used to measure MS by the electron ionization (EI) method. Photoelectron spectroscopic measurement was performed using a JPS-9010C (JEOL) (X-ray source: Mg Kα, pass energy: 30 eV, voltage: 12 kV, current: 5 mA).

A chemiluminescence analyzer Fuji LAS 3000 (Fuji Film), an optical microscope Olympus CKX41 (Olympus), a centrifuge Kubota 6200 (Kubota), an incubator (37 °C, CO_2 5%) (Thermo Steri-Cycle CO_2 incubator), a clean bench Sanyo Class2 typeA/B3 (Sanyo), and a rotary microtome IVS-400 (Sakura Finetek, Japan) were used in cell affinity evaluating test and animal experiment.

2.3. Synthesis of biosilane

Scheme 2 shows the synthetic route.

2.3.1. Synthesis of 1,1-DAU6M

1,1-Diallylurea (3.98 g, 28.4 mmol), THF (10 ml), and 0.1 M chloroplatinic acid hexahydrate solution in THF (0.1 ml) were taken into a 100 ml round bottom flask equipped with a dropping funnel and a reflux condenser and trimethoxysilane (7.22 ml, 56.8 mmol) was added slowly in 30 min in a nitrogen atmosphere to the reaction mixture while heating at its boiling point (ca. 76 °C). The mixture was further heated for 20 h at the boiling point of the mixture. The product was obtained as a colorless transparent liquid after the solvent was removed at a reduced pressure and the residue was distilled in a vacuum (bp 110 °C/40 Pa). The yield was 65% (7.09 g). The spectral data are given in Section 3.1.1.

2.3.2. Synthesis of 1,3-DAU6M

1,3-Diallylurea (1.34 g, 9.57 mmol), THF (10 ml), and 0.1 M chloroplatinic acid hexahydrate solution in THF (0.1 ml), and trimethoxysilane (2.43 ml, 19.1 mmol) were used to synthesize the compound in the same way as in Section 2.3.1. The product was obtained as a colorless transparent liquid (bp 88 °C/10 Pa) in a yield of 82% (3.01 g). The spectral data are given in Section 3.1.2.

2.3.3. Synthesis of MI3M

MI3M was synthesized using maleimide (3.32 g, 34.2 mmol), THF (10 ml), 0.1 m chloroplatinic acid hexahydrate solution in THF

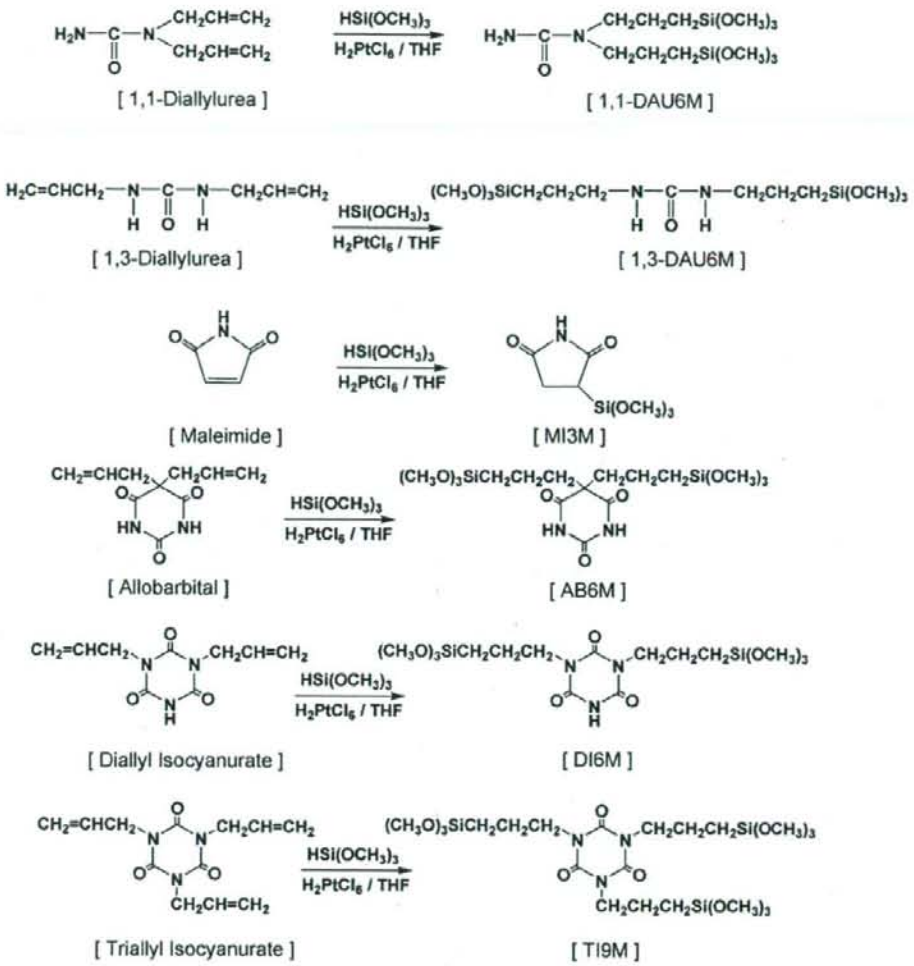

Scheme 2.

(0.1 ml), and trimethoxysilane (4.35 ml, 34.2 mmol) in a similar way to that in Section 2.3.1. The product was obtained as a white solid (bp 105 °C/10 Pa) in a yield of 56% (4.20 g). The spectral data are given in Section 3.1.3.

2.3.4. Synthesis of AB6M

AB6M was synthesized using allobarbital (5.00 g, 24.0 mmol), THF (10 ml), 0.1 M chloroplatinic acid hexahydrate solution in THF (0.1 ml), and trimethoxysilane (6.11 ml, 48.1 mmol) as in Section 2.3.1. The product was obtained as a white solid (bp 250 °C/200 Pa) in a yield of 83% (9.02 g). The spectral data are given in Section 3.1.4.

2.3.5. Synthesis of DI6M

DI6M was synthesized using diallyl isocyanurate (3.00 g, 14.3 mmol), THF (10 ml), 0.1 M chloroplatinic acid hexahydrate solution in THF (0.1 ml), and trimethoxysilane (3.65 ml, 28.7 mmol) as in Section 2.3.1. The product was obtained as a white solid (bp 220 °C/60 Pa) in a yield of 86% (5.59 g). The spectral data are given in Section 3.1.5.

2.3.6. Synthesis of TI9M

TI9M was synthesized using triallylisocyanurate (4.28 g, 17.2 mmol), THF (10 ml), 0.1 M chloroplatinic acid hexahydrate solution in THF (0.1 ml), and trimethoxysilane (6.55 ml, 60.1 mmol) as in Section 2.3.1. The product was obtained as a colorless transparent liquid (bp 205 °C/40 Pa) in a yield of 80% (8.46 g). The spectral data are given in Section 3.1.6.

2.4. In vitro study

2.4.1. Surface modification of cover glass plates

Microcover glass plates were used after being immersed in 1 M aqueous sodium hydroxide for 1 h and in 1 M nitric acid for 1 h, rinsed thoroughly with ion exchanged water, and dried in a vacuum [13]. The cover glasses were then immersed in 10 mM ethanolic

solution of each of the biosilanes for 24 h at room temperature, washed with ethanol, and dried to give biosilane-modified cover glass plates (abbreviated hereafter to modified glass substrates). Modified glass substrates were surface-analyzed using XPS.

2.4.2. Cell viability assay

Modified glass substrates were prepared as in Section 2.4.1 and poly-L-lysine modified cover glass plates as positive control were set in 24-well plates, washed once with ethanol and five times with PBS, and dried. The cell dispersion (400 μl) was placed in each of the 24-well plates and the cells were incubated for 1 h at 37 °C in an incubator. The 24-well plates were then washed twice with PBS and the cells in each plate were observed under the optical microscope. The results are given in Section 3.2.2. PBS (200 μl) and the luciferase assay reagent (200 μl) were prepared as in Section 2.1 and added to each of the well plates and the luminescence from each well plate was detected with the chemiluminescence detecting apparatus after the plates were allowed to stand for 10 min in the dark. The results are given in Section 3.2.3.

2.5. In vivo study

2.5.1. Surface modification of hydroxyapatite and β-TCP

The following experiments were performed to analyze the modified surface by FT-IR. HAp powder (single crystal, 1 g) was placed in 1 mM ethanolic 1,1-DAU6M solution and the mixture was stirred for 24 h at room temperature. The powder was washed five times with 10 ml of ethanol for each washing and dried in a vacuum. The modified HAp powder was surface-analyzed by FT-IR using the KBr tablet method. The results are given in Section 3.3.1.

β-TPC was immersed in 50 mM ethanolic 1,1-DAU6M solution for 24 h at room temperature. The modified β-TPC was dried in the air and sterilized in an ethylene oxide gas atmosphere at 50 °C. β-TPC/osteoblast composite was obtained by incubating the modified β-TPC in the culture medium containing 1×10^6 osteoblasts for 12 h at 37 °C.

2.5.2. Implantation experiment of β-TPC/osteoblast composite using immunodeficient mouse

β-TPC/osteoblast composite together with unmodified β-TPC as control were subcutaneously implanted into the back skin of an immunodeficient mouse and they were taken out 8 weeks later. The implanted samples taken out of the animal were immersed in 4% paraformaldehyde solution at 4 °C for 12 h to fix them (stoppage of tissue denaturation). The fixed samples were washed for 10 min in a running water and the water in the sample tissues was replaced by ethanol and then toluene after being decalcificated in 10% aqueous formic acid solution for 2 days. The samples thus oleophilized were immersed in melted paraffin to allow the liquid to penetrate into them. Then, the samples embedded in paraffin were sliced into 3 μm thick layers with a rotary microtome for histological observation and each layer was dyed with hematoxyline–eosine to be observed under the optical microscope. Positively charged hematoxyline is bound to negatively charged phosphate group of cell nucleus and develops an indigo-blue color while negatively charged eosine is attached to positively charged cytoplasm developing a red or dark red color.

3. Results and discussion

3.1. Synthesis of biosilanes

3.1.1. Synthesis of 1,1-DAUM6M

IR (cm^{-1}) 3346 (ν_{N-H}), 2841–2939 (ν_{C-H}), 1648 ($\nu_{C=O}$), 1057 (ν_{Si-O}); ^1H NMR ($CDCl_3$) δ0.61–0.66 (CH_2Si, t (triplet), 4H; J = 20 Hz), 1.57–1.65 ($CH_2CH_2CH_2$, m (multiplet), 4H), 3.15–3.19 ($N-CH_2$, t, 4H; J = 16 Hz), 3.53–3.57 (CH_3, s (singlet), 18H), 4.63–4.69 (NH_2, s, 2H); MS (*m/z*) (relative intensity with max peak), 384 (4.0) $[M]^+$, 340(22)$[M-CONH_2]^+$, 160(100)$[CH_2CH_2CH_2Si(OCH_3)_3]^+$, 121 (52) $[Si(OCH_3)_3]^+$, 91 (45) $[Si(OCH_3)_2]^+$.

3.1.2. Synthesis of 1,3-DAUM6M

IR (cm^{-1}) 3334 (ν_{N-H}), 2837–2935 (ν_{C-H}), 1628 ($\nu_{C=O}$), 1073 (ν_{Si-O}); ^1H NMR ($CDCl_3$) δ0.63–0.67 (CH_2Si, t, 4H; J = 16 Hz), 1.59–1.63 ($CH_2CH_2CH_2$, m, 4H), 3.13–3.16 ($NH-CH_2$, t, 4H; J = 12 Hz), 3.54–3.57 (CH_3, s, 18H), 4.34–4.49 (NH, s, 2H); MS (*m/z*) (rel int), 384 (12) $[M]^+$, 121 (86) $[Si(OCH_3)_3]^+$, 91 (34) $[Si(OCH_3)_2]^+$.

3.1.3. Synthesis of MI3M

IR (cm^{-1}) 3278 (ν_{N-H}), 2842–2947 (ν_{C-H}), 1716 ($\nu_{C=O}$), 1090 (ν_{Si-O}); ^1H NMR ($CDCl_3$) δ2.75–2.77 (CHSi, s, 1H), 2.78–2.82 (CH_2, d (doublet), 2H; J = 16 Hz), 3.60–3.76 (CH_3, s, 9H), 7.86–8.37 (NH, s, 1H); MS (*m/z*) (rel int), 219 (100) $[M]^+$, 121 (42) $[Si(OCH_3)_3]^+$, 91 (24) $[Si(OCH_3)_2]^+$.

3.1.4. Synthesis of AB6M

IR (cm^{-1}) 3215 (ν_{N-H}), 2842–2951 (ν_{C-H}), 1711 ($\nu_{C=O}$), 1085 (ν_{Si-O}); ^1H NMR ($CDCl_3$) δ0.56–0.60 (CH_2Si, t, 4H; J = 16 Hz), 1.28–1.32 ($CH_2CH_2CH_2$, m, 4H), 1.98–2.02 ($C-CH_2$, t, 4H; J = 16 Hz), 3.53–3.57 (CH_3, s, 18H), 8.11 (NH, s, 2H); MS (*m/z*) (rel int), 451 (3.0) $[M]^+$, 121 (65) $[Si(OCH_3)_3]^+$, 91 (20) $[Si(OCH_3)_2]^+$.

3.1.5. Synthesis of DI6M

IR (cm^{-1}) 3248 (ν_{N-H}), 2847–2946 (ν_{C-H}), 1673 ($\nu_{C=O}$), 1085 (ν_{Si-O}); ^1H NMR ($CDCl_3$) δ0.63–0.67 (CH_2Si, t, 4H; J = 16 Hz), 1.72–1.77 ($CH_2CH_2CH_2$, m, 4H), 3.56–3.60 (CH_3, s, 18H), 3.82–3.85 ($N-CH_2$, t, 4H; J = 12 Hz), 7.95 (NH, s, 1H); MS (*m/z*) (rel int), 453 (4.0) $[M]^+$, 121 (100) $[Si(OCH_3)_3]^+$, 91 (26) $[Si(OCH_3)_2]^+$.

3.1.6. Synthesis of TI9M

IR (cm^{-1}) 2847–2946 (ν_{C-H}), 1689 ($\nu_{C=O}$), 1085 (ν_{Si-O}); ^1H NMR ($CDCl_3$) δ0.63–0.67 (CH_2Si, t, 6H; J = 16 Hz), 1.71–1.75 ($CH_2CH_2CH_2$, m, 6H), 3.56–3.59 (CH_3, s, 27H), 3.82–3.86 ($N-CH_2$, t, 6H; J = 16 Hz);

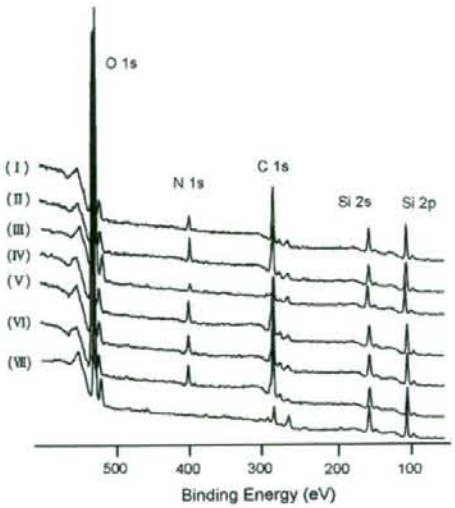

Fig. 1. XPS spectra of glass surfaces modified with 1,1-DAU6M (I), 1,3-DAU6M (II), MI3M (III), AB6M (IV), DI6M (V), and TI9M (VI), and unmodified one (VII).

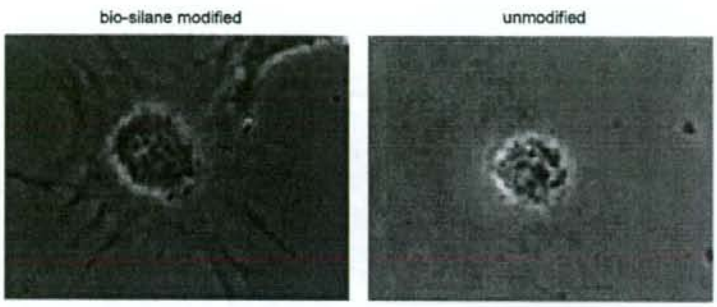

Fig. 2. Photomicrographs of cell adsorption onto biosilane-modified and -unmodified glass surfaces.

MS (*m*/*z*) (rel int), 615 (4.0) $[M]^+$, 121 (100) $[Si(OCH_3)_3]^+$, 91 (18) $[Si(OCH_3)_2]^+$.

3.2. In vitro study

3.2.1. Surface analysis of cover glass

Fig. 1 shows the XPS spectra of glass substrates modified with 1,1-DAU6M, 1,3-DAU6M, MI3M, AB6M, DI6M, and TI9M, together with the spectrum of unmodified glass substrate [14,15]. All substrates exhibited peaks due to Si (2p), Si (2s), C (1s), and O (1s) at around 100, 150, 285, and 530 eV, respectively. In addition, a peak due to N (1s) was observed at around 400 eV for the modified substrates though this peak was not observed for the unmodified substrate, suggesting strongly that the glass substrate was modified with biosilane.

3.2.2. Microscopy

Fig. 2 shows typical optical microscopic images of KUSA cells on the biosilane-modified and unmodified glass substrates. Spherical cells were observed on the modified glass substrate indicating the physically adsorbed cells while somewhat spread cells were observed on the unmodified glass substrate, which shows a high affinity of the cells to the substrate [16].

3.2.3. Relative luminescence intensity

Fig. 3 shows the results of luciferase assay. The luminescence is caused by adenosine triphosphate (ATP) in the cells and its intensity is proportional to cell number [17,18]. Luminescence intensity for the biosilane-modified glass substrates was higher than that for the unmodified substrate, especially the substrates modified with 1,1-DAU6M, 1,3-DAU6M, and AB6M showed an intensity as high as or higher than that for poly-L-lysine-modified glass substrate (poly-L-lysine is a commercially available polymer that exhibits a high affinity to biological cells and used in this work as control). In fact, about 20 times cells were observed on the poly-L-lysine-modified glass substrate when compared with the number of cells on the unmodified substrate. In addition, the intensity of luminescence tended to increase with increasing number of amide groups in biosilane molecule.

3.3. In vivo study

3.3.1. FT-IR spectra of hydroxyapatite modified with 1,1-DAU6M

Fig. 4 shows the FT-IR spectra of 1,1-DAU6M (A), HAp modified with 1,1-DAU6M (B), and unmodified HAp (C). A peak was observed at around 2800 cm^{-1} due to C–H stretching vibration of 1,1-DAU6M in (B). No peak was observed at this wave number in (C), suggesting that HAp was modified with 1,1-DAU6M.

3.3.2. HE stained images

Fig. 5 shows the image of an implanted piece stained with hematoxyline–eosin obtained in the implantation experiment

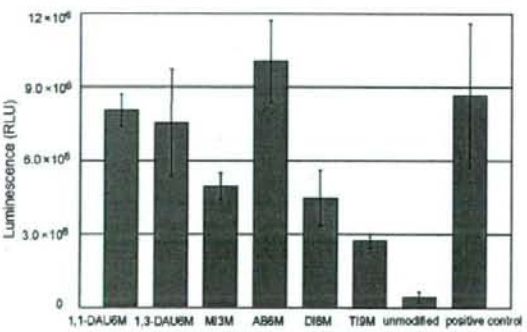

Fig. 3. Relative luminescence intensities of cells adsorbed onto glass surfaces after incubation at 37 °C for 1 h.

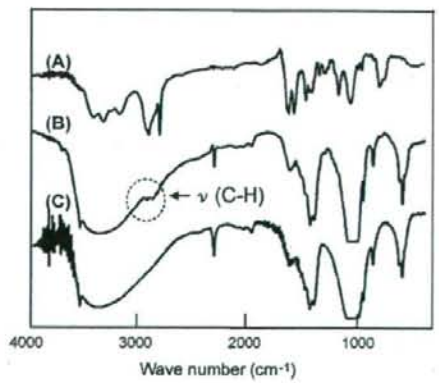

Fig. 4. FT-IR spectra of (A) 1,1-DAU6M monomer, (B) 1,1-DAU6M-modified HAp particle, and (C) unmodified HAp particle.

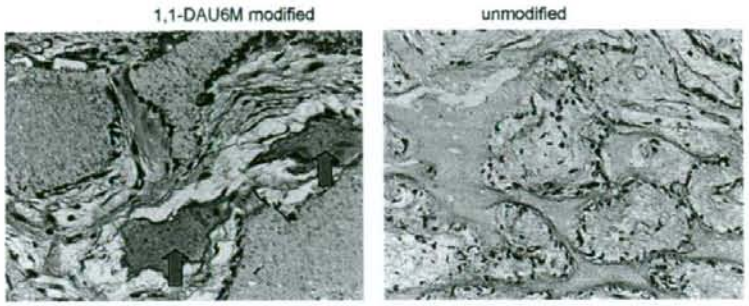

Fig. 5. Hematoxyline–eosin stained images of 1,1-DAU6M modified (two arrows) and unmodified β-TCP/cell composite materials.

using mouse and β-TCP/osteoblast composite. While a bone-like structure was observed in the interior of this composite, no such structure was found for unmodified β-TCP. This would be interpreted as indicating that osteoblasts are hardly fixed on unmodified β-TCP, whereas the cells easily attach to the modified β-TCP through the interaction of amide groups of biosilane on its surface with the cells, thereby making the cells possible to wander into the interior of β-TCP.

4. Conclusions

Six amide group-possessing biosilane were synthesized with the aim to construct the material surface that allows biological cells to be compatible with it. These agents were expected to make a soft landing on cytoplasm without cell destruction through the hydrogen bonding between their amide groups and biological cells. Glass substrates modified with the synthesized biosilanes exhibited a high affinity to biological cells *in vitro*. Very few biological cells were found on the surface of glass substrate modified with silane coupling agent having no amide group. A bone-like structure was observed in the interior of a composite material prepared from β-TCP modified with one of the biosilanes synthesized in this work, 1,1-DAU6M, and osteoblasts in an implantation experiment into an immunodeficient mouse. The biosilanes prepared in this work are expected to greatly contribute to the future bone-regenerating medical treatment.

Acknowledgement

This work was supported in part by Grants-in-Aid for Scientific Research (B) (No. 19390487) from the Ministry of Education, Science, Sports, and Culture of Japan.

References

[1] R. Langer, J.P. Vacanti, Science 260 (1993) 920.
[2] J. Goshima, V.M. Goldberg, A.I. Caplan, Biomaterials 12 (1991) 253.
[3] J.A. Thomson, J. Itskovitz-Eldor, S.S. Shapiro, M.A. Waknitz, J.J. Swiergiel, V.S. Marshall, J.M. Jones, Science 282 (1998) 1145.
[4] J. Song, V. Malaythong, C.R. Bertozzi, J. Am. Chem. Soc. 127 (2005) 3366.
[5] N. Yoshino, Y. Yamamoto, T. Seto, S. Tominaga, T. Kawase, Bull. Chem. Soc. Jpn. 66 (1993) 472.
[6] N. Yoshino, Y. Yamamoto, K. Hamano, T. Kawase, Bull. Chem. Soc. Jpn. 66 (1993) 1754.
[7] N. Yoshino, H. Nakaseko, Y. Yamamoto, React. Polym. 23 (1994) 157.
[8] N. Yoshino, A. Sasaki, T. Seto, J. Fluorine Chem. 71 (1995) 21.
[9] N. Yoshino, Y. Kondo, T. Yamaguchi, J. Fluorine Chem. 79 (1996) 87.
[10] N. Yoshino, T. Teranaka, J. Biomater. Sci., Polym. Ed. 8 (1997) 623.
[11] N. Yoshino, T. Sato, K. Miyao, M. Furukawa, Y. Kondo, J. Fluorine Chem. 127 (2006) 1058.
[12] G.E. Douberly, S. Pan, D. Walters, H. Matsui, J. Phys. Chem. B 105 (2001) 7612.
[13] P. Filippini, G. Rainaldi, A. Ferrante, B. Mecheri, G. Gabrielli, M. Bombace, P.L. Indovina, M.T. Santini, J. Biomed. Mater. Res. 55 (2001) 338.
[14] T.K. Kim, X.M. Yang, R.D. Peters, B.H. Sohn, P.F. Nealey, J. Phys. Chem. B 104 (2000) 7403.
[15] N. Adden, L.J. Gamble, D.G. Castner, A. Hoffmann, G. Gross, H. Menzel, Langmuir 22 (2006) 8197.
[16] C.S. Chen, M. Mrksich, S. Huang, G.M. Whitesides, D.E. Ingber, Science 276 (1997) 1425.
[17] R.L. Klemke, M. Yebra, E.M. Bayna, D.A. Cheresh, Cell Biol. 127 (1994) 859.
[18] A.L. Prieto, G.M. Edelman, K.L. Crossin, Cell Biol. 90 (1993) 10154.

Available online at www.sciencedirect.com

ScienceDirect

Matrix Biology 27 (2008) 232–241

MATRIX BIOLOGY

www.elsevier.com/locate/matbio

Basic fibroblast growth factor regulates expression of heparan sulfate in human periodontal ligament cells

Yoshio Shimabukuro, Tomoo Ichikawa, Yoshimitsu Terashima, Tomoaki Iwayama, Hiroyuki Oohara, Tetsuhiro Kajikawa, Ryohei Kobayashi, Hiroaki Terashima, Masahide Takedachi, Mami Terakura, Tomoko Hashikawa, Satoru Yamada, Shinya Murakami *

Department of Periodontology, Division of Oral Biology and Disease Control, Osaka University Graduate School of Dentistry, 1-8 Yamadaoka, Suita, Osaka 565-0871, Japan

Received 30 March 2006; received in revised form 25 September 2007; accepted 19 October 2007

Abstract

Heparan sulfate (HS) proteoglycan is a widely distributed biological molecule that mediates a variety of physiological responses in development, cell growth, cell migration, and wound healing. We examined the effects of basic fibroblast growth factor-2 (FGF-2), which is known to modulate extracellular matrix (ECM) production of various cell types, on the production of HS proteoglycan by human periodontal ligament (HPDL) cells. We also examined the effects of FGF-2 on the expression of syndecans, a major family of membrane-bound HS proteoglycans. Treatment of HPDL cells with FGF-2 for 72 h resulted in a pronounced increase in the level of HS in the culture supernatant in a dose-dependent manner. However, reverse transcription-polymerase chain reaction data (RT-PCR) revealed that FGF-2 marginally reduced the gene expression of syndecan-1, -2, and -4, and did not alter the level of syndecan-3 mRNA. Furthermore, FGF-2 did not have an effect on the mRNA expression of enzymes associated with HS biosynthesis. Interestingly, FACS analysis revealed that the syndecan family displayed diverse alterations in response to FGF-2. FGF-2 barely altered the expression of syndecan-1, but decreased the expression of syndecan-2 and -4 on HPDL cells. Moreover, dot blot analysis showed that FGF-2 did not alter the level of syndecan-1 and -2, but enhanced the level of syndecan-4 in culture supernatants of FGF-2-stimulated HPDL cells. These results suggest that the FGF-2-activated increase in the level of HS in conditioned medium may be a result of shedding of syndecan-4 from the HPDL cell surface. Taken together, FGF-2 may differentially regulate the expression of HS proteoglycans in a HS-proteoglycan-subtype-dependent manner. The diversity of the expression patterns of HS proteoglycans may be associated with the FGF-2-induced biological functions of HPDL cells.

Keywords: Basic fibroblast growth factor; Heparan sulfate; Periodontal ligament cells; Shedding; Syndecan

1. Introduction

A wide range of extracellular matrix and growth factors participate during the wound-healing process. The basic fibroblast growth factor-2 (FGF-2) is one such growth factor detected in the early phase of wound healing. FGF-2 mediates various biological responses including cellular proliferation, angiogenesis, and tissue repair (Bikfalvi et al., 1997; Nugent and Iozzo, 2000). FGF-2 also modulates the expression of glycosaminoglycans and proteoglycans, as well as collagen and non-collagenous protein, which are main components of connective tissue. However, the details of the regulatory effects of FGF-2 on the expression of glycosaminoglycans and proteoglycans in cells have not been fully defined.

The syndecans are a family of cell surface heparan sulfate (HS) proteoglycans which comprise of a core protein and glycosaminoglycan side chains. Four members of the syndecan family have been identified to date. Whereas syndecan-4 expression is ubiquitous, syndecan-1, -2, and -3 are mainly present in epithelial cells, fibroblasts, and neural cells, respectively. The HS chains of the syndecans are responsible for their biological

* Corresponding author. Tel.: +81 6 6879 2930; fax: +81 6 6879 2934.
E-mail address: ipshinya@dent.osaka-u.ac.jp (S. Murakami).

0945-053X/$ - see front matter © 2007 Elsevier B.V./International Society of Matrix Biology. All rights reserved.
doi:10.1016/j.matbio.2007.10.005

functions, such as extracellular matrix assembly and growth factor binding. The HS chains of syndecans are also known to function as co-receptors of the FGF receptor. It has been reported that when tissue was injured, syndecan expression was increased in epithelial cells, endothelial cells, and fibroblasts (Elenius et al., 1997; Gallo et al., 1996), and shed syndecan ectodomain accumulated in wound fluid (Fitzgerald et al., 2000; Kainulainen et al., 1998; Park et al., 2000). Recent studies have also revealed impaired wound healing in syndecan-deficient mice (Echtermeyer et al., 2001; Ishiguro et al., 2000; Stepp et al., 2002), suggesting an essential role for the syndecans in wound repair.

Periodontal tissue is a tooth-supporting tissue and consists of periodontal ligament, gingiva, cementum, and alveolar bone. The periodontal ligament cells have the potential to secrete a variety of extracellular matrices and support teeth with these molecules. Furthermore, they play key roles in regeneration events following periodontal tissue breakdown caused by progression of periodontal diseases. Interestingly, we revealed that topical application of FGF-2 to periodontal tissue defects activates regeneration of tissue with new cementum and ligament tissue formation (Murakami et al., 1999), which may be a result of FGF-2 increasing cell growth and modulating extracellular matrices. In addition, we explained the stimulatory effects of FGF-2 on the expression of the high molecular type of hyaluronan, a non-sulfated glycosaminoglycan, by human periodontal ligament (HPDL) cells via the up-regulation of hyaluronan synthase (HAS)1 and HAS2 (Shimabukuro et al., 2005). Here we examined the production of HS and the expression pattern of the syndecan gene family by HPDL cells in response to FGF-2.

2. Experimental procedures

2.1. Reagent

Human recombinant FGF-2 was provided by Kaken Pharmaceutical Co., Ltd. (Tokyo, Japan).

2.2. HPDL cells

HPDL cells were isolated from healthy periodontal ligaments of first premolar teeth of individuals undergoing tooth extraction for orthodontic treatment in accordance with the method of Somerman et al. (1988), with minor modifications. All the patients gave informed consent before providing the samples. Healthy periodontal tissue was removed from the center of the root surface with a surgical scalpel. The tissue was minced then transferred to Leighton tubes (Costor, Cambridge, MA, USA). The explants were cultured in α-MEM supplemented with 10% FCS, 50 U/ml penicillin G, and 50 μg/ml streptomycin (henceforth denoted standard medium), with medium changed every 2 or 3 days. Cells were cultured at 37 °C in a humidified atmosphere of 95% air and 5% CO_2. When the cells growing out from the explants had reached confluence, they were separated by treatment with a solution containing 0.05% trypsin and 0.53 mM ethylenediaminetetraacetic acid, collected by centrifugation, and cultured in standard medium in culture dishes until confluency. The cells were then trypsinized and split at a 1:3 ratio. Experiments were carried out with cells from the fourth to fifth passages. In this study, we established 3 cell lines from different volunteers, and all cell lines were used in each experiment. All these cell lines provided similar results in each experiment of this study.

2.3. Reverse transcription-polymerase chain reaction (RT-PCR) for quantitation of mRNA levels

HPDL cells were seeded at a density of 10^5 cells/dish in 600-mm dishes and grown to confluency in standard medium. Following 24 or 48 hours of activation in the absence or presence of FGF-2 (50 ng/ml), total RNA was isolated from HPDL cells by RNAzol™ (Cinna Biotecx Laboratories Inc., Friendswood, TX, USA), according to the manufacturer's instructions. The precipitated RNA was resuspended in 0.1% diethylpyrocarbonate-treated distilled water (DEPC-treated H_2O). This RNA sample was heatdenatured at 65 °C for 10 min and chilled on ice. Complementary DNA (cDNA) synthesis and amplification via PCR were performed as described previously. cDNA synthesis was carried out in a 40 μl reverse transcription mixture containing 52.5 mM Tris–HCl; pH 8.3, 75.5 mM KCl, 3 mM $MgCl_2$, 0.5 mM each dNTPs, 1 mM dithiothreitol, 1.1 U/μl RNase inhibitor (Takara Biomedicals, Shiga, Japan), 55 ng/μl random hexamer, 5 U/μl M-MLV reverse transcriptase (Gibco, Gaithersburg, MD, USA) and RNA. The mixture was incubated at 37 °C for 60 min. At the end of the reverse transcription, all samples were heated at 99 °C for 5 min to inactivate the enzyme and were diluted into 110 μl of DEPC-treated H_2O.

Oligonucleotide PCR primers specific for HS biosynthesis-related enzymes, syndecan-1, -2, -3, and -4, and hypoxanthine phosphoribosyl transferase (HPRT) were synthesized at Takara Shuzo Co. Ltd. (Table 1).

Table 1
Primers utilized for reverse transcription-polymerase chain reaction

Primers	Size		Sequence
HPRT	303 bp	Sense	5′CGAGATGTGATGAAGGAGATGGG3′
		Antisense	5′GCCTGACCAAGGAAAGCAAAGTC3′
GlcNAcT-1	546 bp	Sense	5′CTAAGCTGCAGGGAAATAAA3′
		Antisense	5′TTGCTGTCTGTTGTTTGAAG3′
HS2ST	443 bp	Sense	5′AGGATTTTATCATGGACACG3′
		Antisense	5′TCTTTCCTGTGCGATAGAGT3′
NDST-1	450 bp	Sense	5′ATCTTCTGCCTGTTCAGCGT3′
		Antisense	5′CTCATTGGCCTTGAAGAAGC3′
NDST-2	580 bp	Sense	5′CATGAAGGTGGCTGAGTTG3′
		Antisense	5′CGGATTAAGCAGCACTGTCA3′
Epimerase	624 bp	Sense	5′AGGTGGTTAGGTTGATTGCG3′
		Antisense	5′GCAGTTGATTGATGTGGGTG3′
Syndecan-1	472 bp	Sense	5′CTTTGAAACCCTGGGGAGAATAC3′
		Antisense	5′TCCAGGCAGAAGTCAGAGAAGCAG3′
Syndecan-2	395 bp	Sense	5′GGAGCTGATGAGGATGTAGA3′
		Antisense	5′CACTGGATGGTTTGCGTTCT3′
Syndecan-3	292 bp	Sense	5′GCTTCTTTTCCCTTTACCCTCCGC3′
		Antisense	5′TGTTCCCCAACTTCTCTCTGCCAAG3′
Syndecan-4	245 bp	Sense	5′GGGCAGGAATCTGATGACTTTGAG3′
		Antisense	5′GCTGGACATTGACACCTTGTTGC3′

PCR was performed in a 50 μl mixture containing 5 μl of each sample of derived cDNA, 10 mM Tris–HCl; pH 8.3, 50 mM KCl, 1.5 mM $MgCl_2$, 0.15 mM of each dNTP, 1.25 mM Ampli Taq Gold™ (Perkin Elmer Cetus Co., Emeryville, CA, USA) and 0.2 mM of each primer. After 9 min of predenaturation at 94 °C, PCR was performed in a DNA thermal cycler (MJ Research Inc., Watham, MA, USA) for 21, 24, 27, 30, 33 and 36 cycles to optimize the cycle number to maintain exponential conditions of amplification. Each cycle consisted of denaturation at 94 °C for 45 s, annealing at 56 °C for 45 s, polymerization at 72 °C for 90 s. The 7 μl samples were analyzed on 2% agarose ethidium bromide gels run at 100 V for 25–30 min.

2.4. Determination of the level of HS in culture supernatants

HPDL cells were seeded at a density of 5×10^5 cells in 100-mm culture dishes (Corning Laboratory Sciences Company, Corning, NY, USA) and grown in standard medium. When the monolayers were confluent, the cells were rinsed twice with Hanks' balanced salt solution and incubated in 10% FCS-αMEM in the absence or presence of FGF-2 (1–50 ng/ml). At the end of the incubation periods, the supernatants were collected and stored at −20 °C until determination of HS levels. The HS levels in culture supernatants were measured by an enzyme-linked immunosorbent assay (HS assay kit, Seikagaku Co., Tokyo, Japan), following the manufacturer's instructions. Samples or HS standards were added to the wells which were coated with an anti-HS antibody, and incubated at 4 °C for 24 h. After washing, bound HS was detected by incubating with a biotinylated-antibody specific for HS and horse radish peroxidase (HRP)-conjugated streptavidin for 1 h at room temperature. The plates were washed, loaded with 3,3′,5,5′-tetramethylbenzidene substrate solution and incubated at room temperature before the reaction was stopped with stop solution. Absorbance was measured by a microplate reader (MTP-32; Corona Electric, Hitachinaka, Japan) set at 450 nm/630 nm. The HS levels in samples were calculated from the HS standard curve.

In order to determine the optimal dose of each cytokine for comparison in this study, we preliminarily examined the proliferative responses of HPDL cells induced by the cytokines. A non-saturating dose, which induced nearly equal responses among the cytokines, was selected as an optimal dose of each cytokine in this study. The doses for comparison of FGF-2, epidermal growth factor (EGF), hepatocyte growth factor (HGF), insulin like growth factor-1 (IGF-1), platelet-derived growth factor-BB (PDGF-BB), and transforming growth factor-β (TGF-β) were 50, 100, 50, 50, 50, and 10 ng/ml, respectively.

2.5. Immunocytochemical analysis

HPDL cells were seeded at a density of 5×10^3 cells in 35-mm glass bottom dishes (Matsunami Glass Ind. Ltd., Kishiwada, Japan) and cultured until confluency. At the time of the assay, culture medium was replaced with fresh medium, supplemented with 10% FCS, in the absence or presence of FGF-2 (50 ng/ml). Cells were cultured at 37 °C for the indicated times.

Cell monolayers were fixed with acetone or 2% paraformaldehyde for 10 min, then blocked with 1% bovine serum albumin (BSA) and 10% goat serum in PBS at room temperature for 30 min. The primary antibodies used were: mouse anti-human syndecan-1 antibody (Serotec Ltd., Kidlington, Oxford, UK); goat anti-human syndecan-2 antibody (Santa Cruz Biotechnology Inc., Santa Cruz, California, USA); goat anti-syndecan-4 antibody (Santa Cruz Biotechnology Inc.); mouse monoclonal biotinylated anti-hyaluronan antibody (10E4; Seikagaku Co.). Monolayers were washed three times with PBS to remove unbound antibody, then incubated for 30 min at 37 °C with Alexa Fluor 488-labeled polyclonal anti-mouse or goat IgG antibodies (Molecular Probes, Carlshad, CA, USA) or Alesa Fluor 568-labeled streptavidin (Molecular Probes). The samples were mounted on coverslipped, then viewed using an OLYMPUS 1×70 microscope (Tokyo, Japan) and photographed.

2.6. FACS analysis

HPDL cells were incubated in 10% FCS-αMEM in the absence or presence of FGF-2 (50 ng/ml). At the time of the assay, cells were incubated with mouse anti-human syndecan-1 antibody (Serotec Ltd.), goat anti-human syndecan-2 antibody (Santa Cruz Biotechnology Inc.), and biotin-conjugated mouse anti-syndecan-4 antibody (Santa Cruz Biotechnology Inc.) as primary antibodies. The cells were washed three times with PBS and incubated for 30 min at 37 °C with or without FITC-labeled polyclonal anti-mouse antibody (Caltag Laboratories, Burlingame, CA, USA).

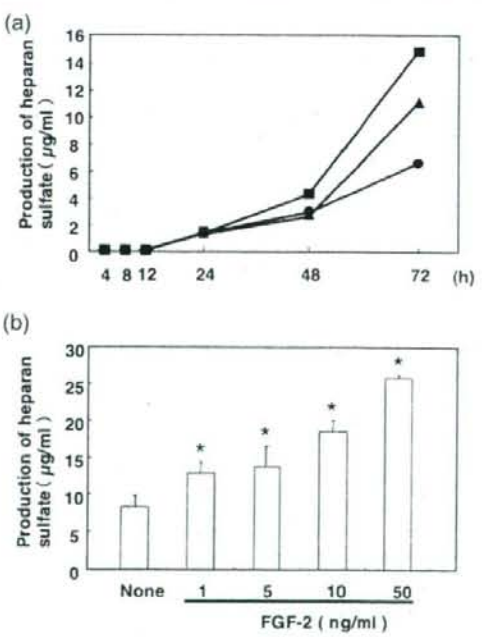

Fig. 1. Effect of FGF-2 on the production of HS by HPDL cells. HPDL cells were cultured in the absence (●) or presence of FGF-2 (5: ▲, 50: ■ ng/ml) and cultured for the indicated times (a.). HPDL cells were cultured in the absence or presence of FGF-2 (1, 5, 10, 50 ng/ml) for 72 h (b.). Conditioned medium was removed and the level of HS analyzed using an enzyme-linked immunosorbent assay. Results of one representative experiment from three separate experiments are shown. (*$p < 0.05$ compared to unstimulated control).

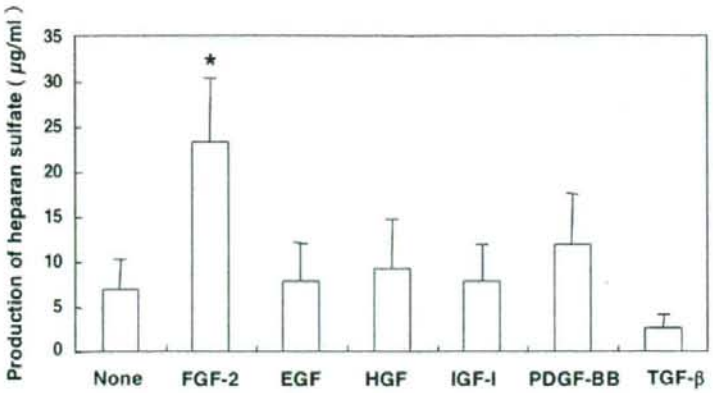

Fig. 2. Effect of various cytokines on HS production by HPDL cells. HPDL cells were cultured without any cytokine or with FGF-2 (50 ng/ml), EGF (100 ng/ml), HGF (50 ng/ml), IGF-1 (50 ng/ml), PDGF-BB (50 ng/ml), or TGF-β (10 ng/ml). Culture supernatants were removed after 72 h of exposure to the various cytokines, and the HS concentration measured by enzyme-linked immunosorbent assay. Results of one representative experiment from three separate experiments are shown. (*$p<0.05$ compared to unstimulated control).

FITC-labeled polyclonal anti-goat antibody (Santa Cruz Biotechnology Inc.), or FITC-labeled streptavidin (BD Biosciences, San Diego, CA).

2.7. Dot blot analysis

Medium from FGF-2-stimulated or unstimulated HPDL cells was collected, and a 400-μl sample spotted onto a nitrocellulose membrane. The membrane was blocked for 1 h with PBS containing 10% BSA, incubated overnight at 4 °C with a mouse monoclonal antibody to syndecan-1, -2, or -4, or a goat polyclonal antibody to glypican-1 (Santa Cruz), -2 (R&D Systems, Inc., Minneapolis, MN, USA), -3 (Santa Cruz), -6 (R&D Systems, Inc.), or perlecan (Santa Cruz), washed with PBS containing 1% BSA, and then incubated with HRP-conjugated rabbit anti-mouse serum or anti-goat serum. Immunoreactive bands were identified using a chemiluminescent kit (ECL, Amersham Pharmacia Biotech, Piscataway, NJ, USA), and were scanned densitometrically and analyzed using NIH image 1.63.

2.8. Statistical analysis

Data are expressed as mean±standard deviation, and were compared by ANOVA and *post-hoc* Scheffé's comparisons.

3. Results

3.1. FGF-2 induced production of HS by HPDL cells, but did not affect the production of HS biosynthesis-associated enzymes

Although FGF-2 has been reported to modulate extracellular matrix production, the effects of FGF-2 on glycosaminoglycan production by HPDL cells have not been fully elucidated (Shimabukuro et al., 2005). Focusing on HS production by HPDL cells, we first analyzed the concentration of HS in conditioned medium of FGF-2-stimulated HPDL cells. HS (1.29 μg/ml) was detected in the culture supernatants after 24 h of stimulation. The concentration of HS was found to gradually increase during 72 h of stimulation, with the increase

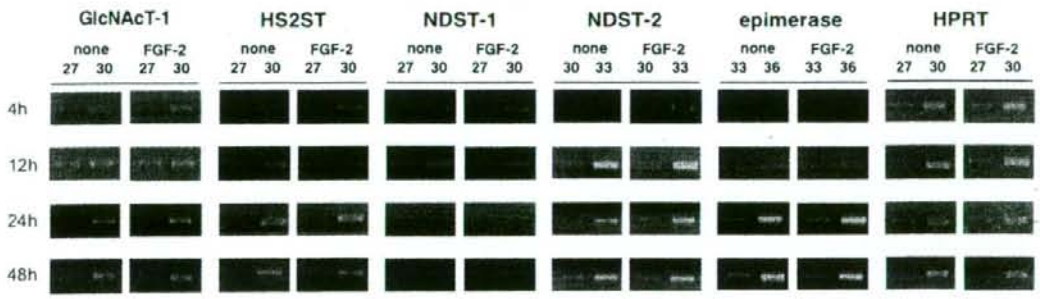

Fig. 3. mRNA expression of HS synthetic enzymes in HPDL cells. The expression of mRNA of HS-related enzymes in HPDL cells cultured in the absence or presence of FGF-2 (50 ng/ml) for 24 h was measured. Total RNA was recovered and RT-PCR performed to analyze the mRNA expression of GlcNAcT-1, HS2ST, NDST-1, NDST-2, epimerase, and HPRT in HPDL cells. Results of one representative experiment from three separate experiments are shown. The number of PCR amplification cycles is shown above each lane.